



CHALMERS

Chalmers Publication Library

Sulfur recirculation for increased electricity production in Waste-to-Energy plants

This document has been downloaded from Chalmers Publication Library (CPL). It is the author's version of a work that was accepted for publication in:

Waste Management (ISSN: 0956-053X)

Citation for the published paper:

Andersson, S. ; Blomqvist, E. ; Bafver, L. (2014) "Sulfur recirculation for increased electricity production in Waste-to-Energy plants". Waste Management, vol. 34(1), pp. 67-78.

<http://dx.doi.org/10.1016/j.wasman.2013.09.002>

Downloaded from: <http://publications.lib.chalmers.se/publication/193133>

Notice: Changes introduced as a result of publishing processes such as copy-editing and formatting may not be reflected in this document. For a definitive version of this work, please refer to the published source. Please note that access to the published version might require a subscription.

Chalmers Publication Library (CPL) offers the possibility of retrieving research publications produced at Chalmers University of Technology. It covers all types of publications: articles, dissertations, licentiate theses, masters theses, conference papers, reports etc. Since 2006 it is the official tool for Chalmers official publication statistics. To ensure that Chalmers research results are disseminated as widely as possible, an Open Access Policy has been adopted. The CPL service is administrated and maintained by Chalmers Library.

(article starts on next page)



Sulfur recirculation for increased electricity production in Waste-to-Energy plants [☆]



Sven Andersson ^{a,*}, Evalena W. Blomqvist ^b, Linda Bäfver ^{b,1}, Frida Jones ^b, Kent Davidsson ^b, Jan Froitzheim ^c, Martin Karlsson ^a, Erik Larsson ^c, Jesper Liske ^c

^a Götaverken Miljö AB, Box 8876, SE-402 72 Göteborg, Sweden

^b SP Technical Research Institute of Sweden, Box 857, SE-501 15 Borås, Sweden

^c High Temperature Corrosion Centre, HTC, Chalmers University of Technology, SE-412 96 Göteborg, Sweden

ARTICLE INFO

Article history:

Received 1 March 2013

Accepted 4 September 2013

Available online 17 October 2013

Keywords:

Sulfur

Dioxins

Superheater

Corrosion

Waste incineration

ABSTRACT

Sulfur recirculation is a new technology for reducing boiler corrosion and dioxin formation. It was demonstrated in full-scale tests at a Waste to Energy plant in Göteborg (Sweden) during nearly two months of operation. Sulfur was recirculated as sulfuric acid from the flue gas cleaning back to the boiler, thus creating a sulfur loop.

The new technology was evaluated by extensive measurement campaigns during operation under normal conditions (reference case) and operation with sulfur recirculation. The chlorine content of both fly ash and boiler ash decreased and the sulfur content increased during the sulfur recirculation tests. The deposit growth and the particle concentration decreased with sulfur recirculation and the dioxin concentration (I-TEQ) of the flue gas was reduced by approximately 25%. Sulfuric acid dew point measurements showed that the sulfuric acid dosage did not lead to elevated SO₃ concentrations, which may otherwise induce low temperature corrosion.

In the sulfur recirculation corrosion probe exposures, the corrosion rate decreased for all tested materials (16Mo3, Sanicro 28 and Inconel 625) and material temperatures (450 °C and 525 °C) compared to the reference exposure. The corrosion rates were reduced by 60–90%. Sulfur recirculation prevented the formation of transition metal chlorides at the metal/oxide interface, formation of chromate and reduced the presence of zinc in the corrosion products. Furthermore, measured corrosion rates at 525 °C with sulfur recirculation in operation were similar or lower compared to those measured at 450 °C material temperature in reference conditions, which corresponds to normal operation at normal steam temperatures. This implies that sulfur recirculation allows for higher steam data and electricity production without increasing corrosion.

© 2013 The Authors. Published by Elsevier Ltd. All rights reserved.

1. Introduction

Today, electricity production in waste to energy plants is limited by the maximum achievable temperature in the superheaters, above which the corrosion rate becomes impractically high.

Abbreviations: A, Alkali = Na and K; Cl/S, Chlorine/sulfur molar ratio; DLPI, Dekati Low-Pressure Impactor; EDX, Energy Dispersive X-rays; ICP-AES, (Inductively Coupled Plasma-Atomic Emission Spectrometry); ICP-OES, (Inductively Coupled Plasma-Optical Emission Spectrometry); I-TEQ, International Toxic Equivalents; PCDD, Polychlorinated dibenzo-p-dioxins; PCDF, Polychlorinated dibenzofurans; SEM, Scanning Electron Microscopy; TEF, Toxic Equivalent Factor; XRD, X-Ray Diffraction.

[☆] This is an open-access article distributed under the terms of the Creative Commons Attribution-NonCommercial-No Derivative Works License, which permits non-commercial use, distribution, and reproduction in any medium, provided the original author and source are credited.

* Corresponding author. Tel.: +46 31 501981; fax: +46 31 229867.

E-mail address: sven.andersson@gmab.se (S. Andersson).

¹ Current address: Pöyry SwedPower AB, P.O. Box 1002, SE-405 21 Göteborg, Sweden.

Usually a steam temperature of 400 °C, corresponding to a material temperature of 425–450 °C, is used, but some newer plants are designed for slightly higher temperatures. This paper aims at increasing the steam temperature to 500 °C. The purpose of the novel sulfur recirculation process, described in Section 1.1, is to reduce the corrosion rate of the superheaters in waste to energy plants by recirculating sulfur from the wet flue gas cleaning back to the boiler. The recirculated SO₂ reacts with the chloride containing ashes and deposits as described in Section 1.2, creating sulfates, which are less sticky than chlorides. Ashes with less chlorides produce less dioxins and less superheater corrosion (Sections 1.3 and 1.4). The long-term aim is higher electricity efficiencies in biomass and waste fired boilers using sulfur recirculation.

1.1. Sulfur recirculation

The purpose of this study is to demonstrate how the sulfur in the fuel can be recirculated in a full scale plant in order to achieve

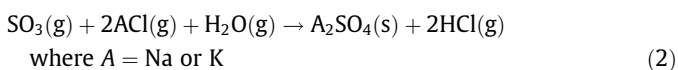
less corrosive deposits in Waste-to-Energy plants. The recirculated sulfur will increase the gas concentration of SO₂ in the boiler and decrease the Cl/S ratio of the deposits and ashes, thus producing a less corrosive environment for the superheaters (Hunsinger et al., 2006, 2007). The innovative, patented sulfur recirculation process, for which Götaverken Miljö AB has a world-wide exclusive license, was invented by Hans Hunsinger at Karlsruhe Institute of Technology (KIT) and has previously been tested in the 0.5 MW waste incineration pilot plant “TAMARA” at KIT. The proposed technology is unique in the way that it, contrary to other methods, only uses the existing sulfur in the fuel and does not increase the amount of residues produced.

1.2. The influence of sulfur on ashes and deposits

The formation of deposits is more pronounced in waste incineration compared to combustion of most other fuel. One reason is the high content of chlorine, alkali (sodium and/or potassium) and ash in waste. During incineration, most of the chlorine enters the gas phase (Bøjer et al., 2008; Lang et al., 2006). Some of it reacts with alkali to form volatile alkali chlorides (Miles et al., 1996; Olsson et al., 1997) and the rest is HCl(g). In the furnace, alkali chlorides are mainly gaseous, but form submicron particles (size < 1 μm) when the gas is cooled in the boiler. The gaseous and particulate alkali chlorides are deposited on the heat transfer surfaces where they may cause corrosion. Sulfur may react with alkali chlorides to form alkali sulfates by so called sulfation. Addition of sulfate and sulfur has been shown to decrease the chlorine content in the deposits during co-firing of straw pellets and wood pellets in a fluidised bed (Davidsson et al., 2008). During co-firing of bark and peat, an increase in deposits was found at Cl/S > 0.15 (Theis et al., 2006). By increasing the sulfur content in the fuel, the chlorine content of the deposits may be reduced (Robinson et al., 2002). In flue gases from incineration, sulfur is mainly present as SO₂ and a minor fraction (typically a few percent) as SO₃ which is described by the equilibrium and reaction rate of:

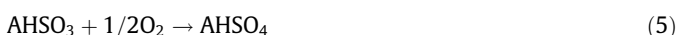


Alkali chlorides react readily with SO₃ according to:



(Iisa et al., 1999; Glarborg and Marshall, 2005)

According to Hunsinger et al. (2007), alkali chlorides also react with SO₂. Hindiyarti et al. (2008) have studied the reaction of alkali chlorides with SO₂ in an entrained flow reactor and propose the following reactions based on detailed kinetic modeling:



1.3. The influence of sulfur on dioxins

It has been shown in numerous laboratory, pilot- and full-scale studies that the presence of sulfur in the flue gas reduces the amount of dioxins (I-TEQ) emitted (Chang et al., 2006; Gullett et al., 1992, 2000; Hunsinger et al., 2003, 2006, 2007; Lindbauer and Wurst, 1992; Ogawa et al., 1996). Two possible theories behind the phenomena are often discussed viz.:

- (1) Due to the presence of SO₂ in the flue gas the equilibrium between Cl₂ and HCl is shifted towards the inactive form (HCl) (Griffin, 1986; Wikström et al., 2003)
- (2) Metal chlorides, especially CuCl₂, which promote the reaction rate of the de novo synthesis of dioxins, react with sulfur to form inactive metal sulfates (Ryan et al., 2006; Gullett et al., 1992).

Experiments in full scale have shown that the inhibition effect of sulfur lasts for several hours (Hunsinger et al., 2007); a finding that indicates that the role of metal chlorides and the de novo synthesis (theory 2 above) is important.

1.4. The influence of sulfur on corrosion

It is well known that waste-fired plants are affected by more serious corrosion problems compared to coal-fired boilers. The higher corrosion rate can be related to differences in the combustion environment: less sulfur-containing compounds, higher concentrations of water vapor and HCl in addition to an increased amount of alkali compounds, especially alkali chlorides. Laboratory investigations of the initial corrosion attack have shown the following:

- Water vapor and oxygen react with chromium oxide to form a compound which evaporates so that chromium is depleted from the metal surface. Since chromium is necessary to form a protective oxide layer on FeCr steels this protection is inhibited and the metal surface is subject to rapid corrosion (Asteman et al., 1999; Halvarsson et al., 2006; Segerdahl et al., 2002; Froitzheim et al., 2010).
- The breakdown of the protective oxide on FeCr steels does also occur in the presence of alkali chlorides. In this case, the chromium rich and protective oxide is converted into alkali chromate (e.g. K₂CrO₄) and poorly protecting Fe₂O₃, resembling the corrosion properties of low alloyed steels (Pettersson et al., 2005; C. Pettersson et al., 2006; Segerdahl et al., 2004; Jonsson et al., 2009)
- On low alloyed steels, the presence of alkali chlorides increases the corrosion rate by the formation subscale transition metal chlorides, causing an increased ionic transport through the oxide and poor scale adhesion (Folkesson et al., 2011; Jonsson et al., 2011).

The good resistance towards high temperature corrosion which characterizes high temperature materials is due to the ability to form oxides which inhibits further oxidation and corrosion. Stainless steels are a group of materials which are often used in the more corrosive parts of the boiler. These steels will at high temperatures form a protective oxide, consisting of both iron and chromium, on the form (Fe_xCr_{1-x})₂O₃ (i.e. a solid solution of chromium (III) oxide (Cr₂O₃) and iron (III) oxide (Fe₂O₃)). The protective properties of this oxide depend on the chromia content, where oxides with a high Cr/Fe ratio are more protective. Hence, processes that deplete the oxide in chromium tend to be harmful, leading to an iron rich oxide with poor protective properties. With biomass or waste as fuel, such processes are related to the high concentrations of alkali compounds and water vapor, forming alkali chromate and gaseous chromic acid, respectively, and a poorly protective oxide layer.

It has been shown that the corrosive effect of alkali chlorides and water vapor can be suppressed by increasing the presence of sulfur-containing compounds in the corrosive environment. Pettersson et al. (2011) have shown how the protective chromium rich oxide layer of the austenitic stainless steel 304L can react with KCl and K₂CO₃ to form K₂CrO₄ which is non-protective. K₂SO₄,

however, does not react in this way. Thus, by converting corrosive alkali chlorides and alkali carbonates in the deposits of the superheaters to stable alkali sulfates, the corrosion attack is greatly reduced. It has also been shown that relatively low concentrations of SO₂ (<100 ppm) inhibits the oxidation of several FeCr steels at temperatures up to 600 °C (Jardnas et al., 2001, 2008).

The beneficial effect of adding sulfur or sulfur-rich additives to biomass and waste fired boilers in order to decrease the high temperature corrosion have been studied earlier (J. Pettersson et al., 2006; Brostrom et al., 2007; Folkesson et al., 2008; Viklund et al., 2009; Kassman et al., 2013). In contrast to the current paper, all these studies have been performed in FB-boilers with additives added from external sources.

2. Materials and methods

The sulfur recirculation process was tested in full-scale for nearly two months accompanied by an extensive measurement and sampling program.

2.1. Full scale tests

Full scale tests were performed at the Waste-to-Energy plant Renova in Göteborg (Sweden), which consists of four lines for incineration of waste. The tests were performed at line P5, which is a grate-fired furnace with a waste throughput of 22 tons/h, shown in Fig. 1. The flue gas cleaning system consists of an ESP (Electrostatic Precipitator) for removal of fly ash, an economiser for district heat production, a two-stage wet scrubber for HCl and SO₂ removal, a condensing scrubber for enhanced energy recovery, a reheater and finally a bag house filter with activated carbon injection.

Two measurement campaigns, each of approximately 1000 h, were performed during normal operation and during sulfur recirculation. These are denoted Ref and Recirc, respectively. Before the recirculation tests were carried out, three different levels of recirculation were tested during an optimization phase, denoted Opt. The results from these optimization measurements were used to find optimal conditions for the 1000 h-test.

An extensive program of samplings and measurements were performed both during the Ref and Recirc in order to assess various aspects of operational differences. Corrosion, deposits and particle

measurements were made immediately upstream of the first superheater. The material temperatures of the corrosion and deposit probes were 450 and 525 °C respectively in order to represent both current material temperatures of superheaters as well as future temperatures in boilers with advanced steam data. ESP ash (fly ash) and boiler ash were sampled and analyzed in order to quantify the sulfation. Acid dew point measurements were performed upstream of the economiser (denoted Eco in Fig. 1). Dioxin sampling was made downstream of the economiser, upstream of the scrubber quench. Emission measurements were made before the stack in order to exclude any negative side effects from sulfur recirculation.

2.2. Sulfur recirculation system

Normally, the second scrubbing stage operates with NaOH as desulfurization agent. During these tests, H₂O₂ (hydrogen peroxide) was used instead, which reacts readily with SO₂ and forms H₂SO₄ (sulfuric acid).



The sulfuric acid produced in the scrubber is injected into the furnace through 6 lances with atomization air, surrounded by recirculated flue gas in order to improve mixing over the cross section. The temperature in the furnace is approximately 1000 °C at the injection level, leading to a rapid decomposition of H₂SO₄ to SO₂.



The resulting high concentration of SO₂ in the boiler reacts with the corrosive alkali chlorides to produce non-corrosive alkali sulfates (Hunsinger et al., 2007) as described in Sections 1.2 and 1.4.

2.3. Acid dew point measurements

The acid dew point was measured using a "Lancom 200 Acid Dewpoint Monitor" from LAND Instruments International. The measurements were performed downstream of the ESP, but before the economiser, since this is where metallic construction materials are used at the lowest temperatures. The instrument consists of a probe with two platinum electrodes incorporated in a

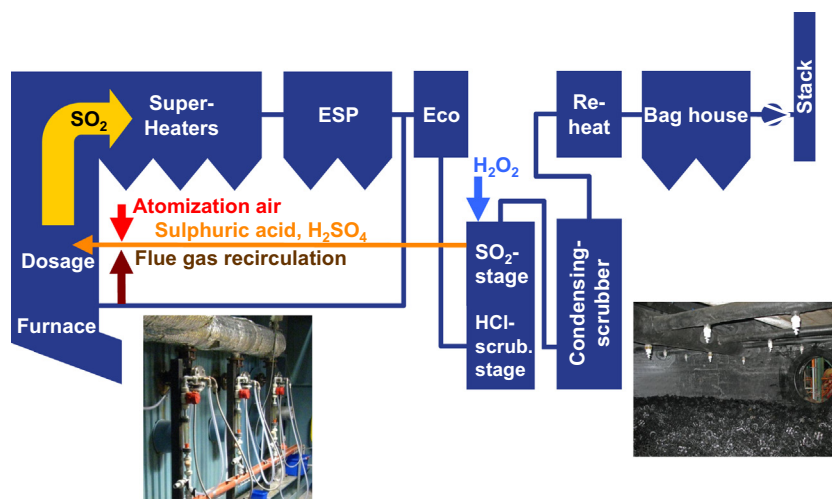


Fig. 1. The sulfur recirculation system at the Renova Waste-to-Energy plant consists of a hydrogen peroxide dosage system and a system for sulfuric acid recirculation using atomization air and flue gas recirculation. The photographs show three of the injection lances (left) and the tower packings and spray lances of the desulfurisation stage (right).

temperature-controlled quartz surface. By cooling the probe with pressurized air, the desired temperature was maintained. In case the temperature is below the acid dew point, sulfuric acid would condensate onto the quartz surface leading to a measurable current in the μA range.

2.4. Particles deposits and ashes

2.4.1. Particle size distribution measurements

Particle size distribution measurements were performed upstream of the first superheater (Fig. 1) with a Dekati Low Pressure Impactor (DLPI) connected to a quench/dilution (Q/D) probe (Johansson et al., 2008). At this spot, the flue gas is about 600 °C. The Q/D probe is used to sample solid particulate material and inorganic vapors, which are quickly nucleated to fine particles, less than 1 μm in size. The extracted gas was diluted eight times in the probe and cooled to 105 °C before entering the DLPI (also heated to 105 °C). The particles in the extracted gas were separated by impaction into 13 sizes ranging from 0.03 μm diameter to 10 μm . Flue gas was sampled for 5–15 min, and the collected mass of each particle size was subsequently put in desiccators and weighed. Chemical analysis was thereafter performed on the fine particles <1 μm and on the large particles >1 μm resulting in the elemental composition of fine (originating from vapor compounds) and large particles (fragments from the fuel) respectively.

2.4.2. Deposit rate probes

Deposit probes were used to simulate heat transfer tubes. Deposits were collected on steel rings (Sandvik Sanicro 28) fitted on cooled probes and exposed to the flue gas in the same position where particle size measurements were carried out. Apart from the heating up (5–10 min), the surface temperatures of the rings were kept constant at 450 °C and 525 °C, respectively. The duration of the exposure to flue gas was 2 h in most cases. The deposits were weighed and chemically analyzed with respect to elemental composition.

2.4.3. Ash sampling

Fly ash was sampled from the ESP directly downstream of the main ash conveyer. Boiler ash was sampled at the ash conveyer from two out of three hoppers (including first draught and superheaters, but excluding ash from the economiser).

2.5. Dioxin sampling

Dioxin sampling of the flue gas was performed by an AMESA continuous dioxin sampling system, certified according to EN1948 (Becker et al., 2000). Both gaseous and particulate phase were collected isokinetically. The sampling system consists of a probe, a XAD II adsorbent cartridge followed by a cooling, drying, measuring and pumping unit. Münster Analytical Systems in Münster, Germany performed the analyses.

2.6. Corrosion measurements

2.6.1. Materials used

An overview of the tested materials, including the standard designation and typical chemical compositions, are given in Table 1. All materials are iron-based except Inconel 625 which is a nickel-based steel welded onto a 16Mo3 substrate.

2.6.2. Corrosion probe

Fig. 2 shows a schematic of the corrosion probe. The six sample rings were mounted on the isothermal probe in the order shown in Fig. 2. The temperature was measured using three thermocouples which were mounted in the metal goods, and directed against

Table 1
Chemical composition of the tested materials in weight%.

	% C	% Fe	% Cr	% Ni	% Mo	Other
16Mo3	0.12	99	–	–	0.3	0.6% Mn
Inconel 625	<0.10	5	22	58	9	0.5% Mn
Sanicro 28	<0.02	35	27	31	3.5	1% Cu

the flue gas. The probe was cooled by compressed air being fed from a PID-controlled valve. The samples consisted of rings with a diameter of 38 mm and 33 mm in length. The wall thickness was 4 mm.

2.6.3. Preparation of material samples

Before exposure, the sample rings were washed with acetone and then with ethanol in an ultrasonic bath. All samples were weighed and stored in plastic bottles until the assembly of the probe. To calculate the material loss from the samples, the sample thickness was measured before and after exposure.

2.6.4. Corrosion analysis

After exposure, the sample rings were inspected optically and weighed, giving an indication of the amount, color, thickness and adhesion of deposit and corrosion product layer. The samples were cast in epoxy, cut and polished in order to study the deposit and corrosion products in the cross-section. These cross-sections were analyzed with SEM/EDX, which gives information about where different elements and phases are located in the deposits and corrosion products. All analyses were done on the wind side of the sample rings unless otherwise stated.

2.6.4.1. Corrosion rate. To determine the material loss the thickness of the samples was measured with micrometer screw before the exposure. The micrometer screw had a round measuring surface for the best measurement of curved objects. The sample thickness was measured at eight points evenly distributed around the mantle surface. The hole for the thermocouple, which was located on the windward side, was in the middle between the first and the last measuring point. After exposure the samples were cut and the wall thickness was measured with an optical microscope. The material loss rate was calculated by the difference between the two measured thicknesses. In order to eliminate systematic errors unexposed samples were measured with both micrometer screw and optical microscope. The measured measurement error in the corrosion rate was 0.02 $\mu\text{m}/\text{h}$. No systematic error was detected when the two methods were compared.

2.6.4.2. SEM imaging. The sample rings were cast in epoxy and cut in a precision saw. The cut side was polished with 220, 500, 1000, in 2400 and 4000 SiC paper and then polished with 1 μm diamond paste. All the cutting and grinding were carried out without the presence of water. The polished cross-sections were analyzed using scanning electron microscopy (SEM).

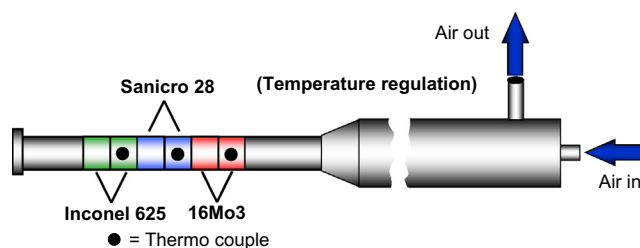


Fig. 2. Schematic image of the corrosion probe.

The resolution and focus depth in an SEM is much higher compared to an ordinary optical microscope. Furthermore, the electron microscope (in contrast to the optical microscope) can provide information about the elemental composition of the sample using backscattered electrons (BSE) or X-rays. Within this project, the chemical composition of each sample was analyzed in the SEM using Energy dispersive X-ray fluorescence (EDX). EDX element maps show the distribution of various elements in the image. These maps were supplemented by EDX quantification, providing the composition of the sample in each point. The lateral resolution for imaging and analysis depends on the acceleration voltage and composition but is typically 0.5 μm for BSE and 1 μm for EDX at 20 kV (used for SEM imaging and analysis).

3. Results and discussion

3.1. Sulfur recirculation

Sulfur recirculation was successfully operated during nearly two months. The resulting mean gas concentrations of HCl and SO_2 in the boiler during 1000 h of operation in Ref and 1000 h in Recirc are shown in Table 2. The emission data collected by the plant's continuous analysers showed no significant increase of any pollutants as seen in Table 3. The SO_2 stack concentration increased from 1.0 to 1.5 mg/Nm^3 (dry gas, 11% O_2) during recirculation, which is only 3% of the emission limit. NH_3 emissions were significantly reduced due to the lower pH-value in the desulfurisation scrubber stage during sulfur recirculation.

In Fig. 3, the response of SO_2 to stepwise changes of dosage of sulfuric acid is shown. Fig. 4 demonstrates how the SO_2 concentration downstream of the boiler can be kept nearly constant using a control loop for sulfuric acid dosage (right), although the sulfur concentration in the waste varies (left).

The sulfur recirculation increases and stabilizes the SO_2 concentration, without causing any risk for exceeding the emission limits, and it has been shown to function over extended time periods.

3.2. Acid dew point measurements

Sulfuric acid dew point measurements were performed during several weeks with a total of approximately 75 h. The probe temperature was varied between 80 $^\circ\text{C}$ and 200 $^\circ\text{C}$ and no current was detected, which means that no sulfuric acid droplets were formed on the probe. At probe temperatures around 60 $^\circ\text{C}$, water condensed on the probe, resulting in a current reading. According to the instrument manufacturer, the detection limit is 110–

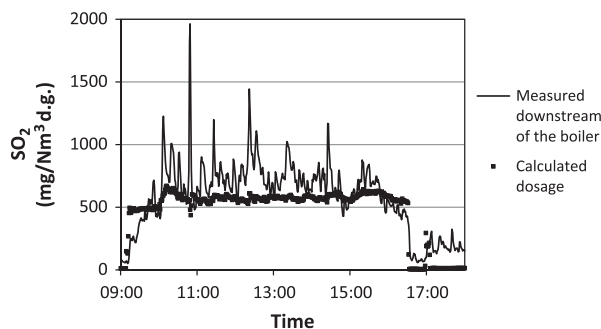


Fig. 3. Step response for the SO_2 concentration downstream of the boiler from a constant flow of sulfuric acid into the furnace, given as calculated SO_2 concentration.

120 $^\circ\text{C}$, which means that the acid dew points during these tests were always lower. The measurements showed that the sulfuric acid dosage did not lead to elevated SO_3 concentrations, which may otherwise lead to low temperature corrosion.

3.3. Particles, deposits and ashes

3.3.1. Particle size distributions

Mass size distributions of particles are shown in Figs. 5 and 6, in four reference cases and four recirculation cases, respectively. Dashed lines and error bars indicate that the sampling is not isokinetic for large particles ($>1 \mu\text{m}$) (Johansson et al., 2008). The total particle mass and the mass of fine particles ($<1 \mu\text{m}$) decreased approximately by a factor of two during recirculation. Theoretically, sulfation of pure particulate NaCl increases the mass by 21% and the total mass of particulates is thereby estimated to increase by a few percent. The fine particles are assumed to have been formed by nucleation from gaseous species. This shows that the recirculation has decreased the amount of species likely to nucleate during the cooling of the flue gas. The recirculation should therefore lead to less deposits on superheater tubes, which is positive for the boiler performance and possibly also lowers the corrosion rate. The chemical composition of the fine particles does not differ significantly between the reference case and the recirculation. Most of the fine particles consist of alkali and chloride with some sulfate. The particle measurements were performed during comparatively short periods: about 10 min. The composition of the fuel combusted at those measurements is unknown but may affect the composition of the particles.

Table 2

Mean values of HCl concentration downstream of the boiler (calculated from HCl scrubber discharge), calculated SO_2 dosage into the boiler and SO_2 concentration downstream of the boiler during the 1000 h reference run and 1000 h sulfur recirculation run (1 atm, 0 $^\circ\text{C}$, dry gas).

	HCl downstream of the boiler (calculated) (mg/Nm^3) (d.g.)	SO_2 injected into the boiler (calculated) (mg/Nm^3) (d.g.)	SO_2 downstream of the boiler (measured) (mg/Nm^3) (d.g.)
Ref	890	0	270
Recirc	1050	460	720

Table 3

Mean values of emissions during the 1000 h reference run and 1000 h sulfur recirculation run together with the 24-h emission limits. All concentrations refer to 1 atm, 0 $^\circ\text{C}$, dry gas and 11% O_2 .

	HCl (mg/m^3)	SO_2 (mg/m^3)	NH_3 (mg/m^3)	NO_x (mg/m^3)	CO (mg/m^3)	TOC (mg/m^3)	CO_2 vol% d.g.	O_2 vol% d.g.
Emission limit	10	50	10 ^a	200	50	10		
Ref	3.8	1.0	1.3	49	15	0.2	10.5	8.6
Recirc	3.7	1.5	0.18	54	4.7	0.2	10.5	8.7

^a Guideline value.

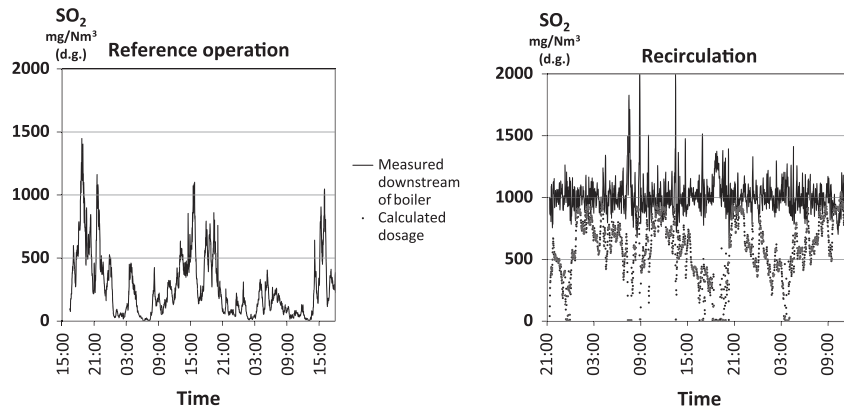


Fig. 4. During normal operation (left), the SO_2 concentration is characterized by large fluctuations. With sulfur recirculation (right), the SO_2 concentration downstream of the boiler was kept constant by controlling the sulfuric acid dosage, given as calculated SO_2 concentration.

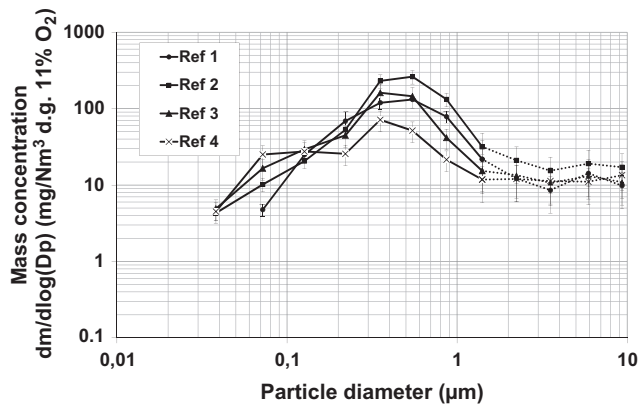


Fig. 5. Mass size distribution in the four reference measurements. At particle sizes larger than $1 \mu\text{m}$, the mass concentrations are shown with dashed lines and error bars because of the larger uncertainty in this region.

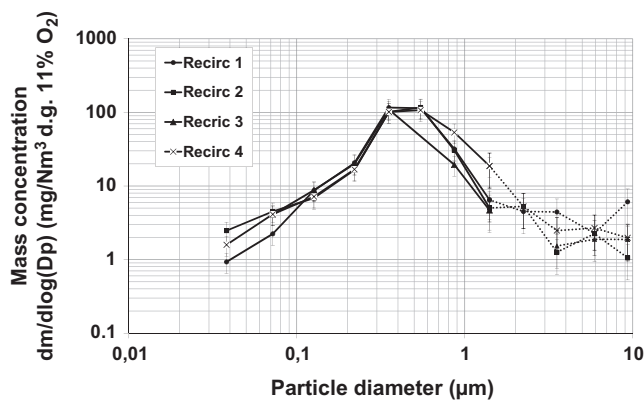


Fig. 6. Mass size distribution in the four recirculation measurements. At particle sizes larger than $1 \mu\text{m}$, the mass concentrations are shown with dashed lines and error bars because of the larger uncertainty in this region. In Recirc 3, one measurement point is missing.

3.3.2. Deposit formation

The growth rate of deposits vs. concentration of SO_2 downstream of the boiler is shown in Fig. 7. The deposit rate decreases with SO_2 concentration in the Ref measurements as well as in all 450°C measurements. Even though the variations are very large for the Recirc 525°C measurements, the mean deposit rate is

clearly lower at higher SO_2 concentrations. Furthermore, all deposit rates at higher SO_2 concentrations were lower or similar than at the lowest SO_2 concentration which represents the mean value of Ref operation. This is in accordance with the purpose of sulfur recirculation; i.e. to sulfate alkali chlorides and thereby making alkali less sticky, which should result in less deposition. As expected from the particle analysis (cf. Section 3.3.1) the growth rate, on average, is lower during the recirculation case than during the reference. However, the variation is large, especially during the recirculation cases. Most expositions lasted for 2 h but one was exposed 3 h 16 min and the short runs lasted for 6–19 min. Most notably, the shortest exposure (6 min) gave the highest deposit of all Recirc 450°C measurements ($47 \text{ g/m}^2, \text{h}$). It is also shown that the growth rate is higher at a surface temperature of 525°C . The reason for this may be that the material that deposits on the surface is stickier, and thereby favors further deposition.

3.3.3. Ash composition

Due to the higher sulfation rates at increased SO_2 concentrations, the Cl/S ratio decreased with SO_2 concentration for both fly ash and boiler ash, as shown in Fig. 8. During the optimization phase preceding the actual test run, it was concluded from the fly ash measurements that an SO_2 concentration of approximately $800 \text{ mg/Nm}^3 \text{ (d.g.)}$ would yield significantly lower Cl/S ratios compared to normal operation at a few hundred $\text{mg/Nm}^3 \text{ (d.g.)}$.

The increased sulfation of the ashes, resulting from sulfur recirculation, leads to a molar flow rate of sulfur in the ashes comparable to the molar flow rate of SO_2 from the waste. This means that there is a potential for waste sulfate water free operation, eliminat-

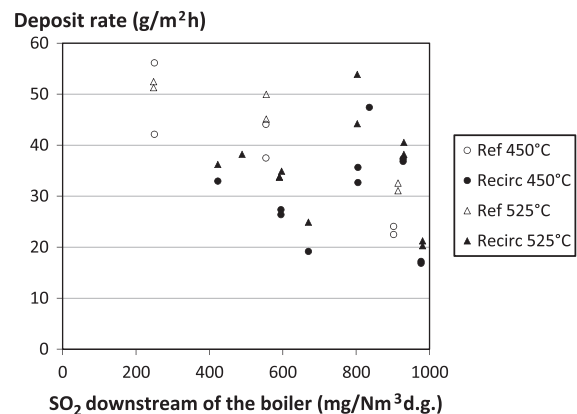


Fig. 7. Growth rate of deposition vs. SO_2 concentration downstream of the boiler.

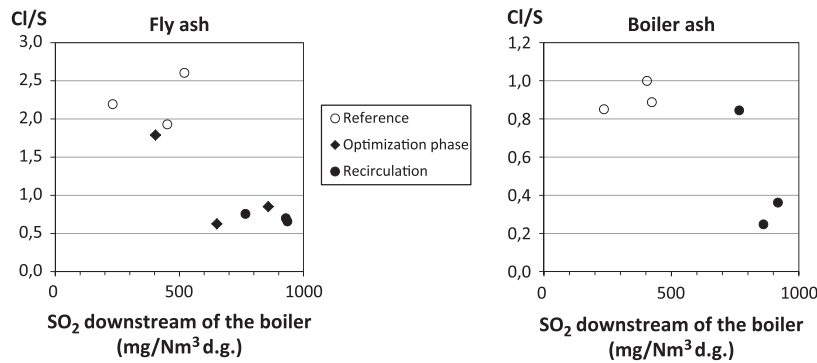


Fig. 8. The molar Cl/S ratio in the ashes as a function of the SO₂ concentration downstream of the boiler from the reference (○), optimization (◆) and sulfur recirculation (●) cases.

ing the need for a gypsum precipitation process. The amount of HCl released from the sulfation is small compared to the normal HCl concentration in the gas, but leads to a small increase in chlorides released with the effluent water, which is normally discharged to the sea. The composition and amount of bottom ash is not changed since the recirculated sulfur is injected downstream of the furnace.

3.4. Dioxins

In total, dioxins (I-TEQ) were measured in seven flue gas samples and four ash samples. Four of the flue gas samples and two ash samples were taken without sulfur added and the rest with sulfur recirculation applied. Fig. 9 presents the measured I-TEQ levels in the seven flue gas samples. An average of 1.34 ng I-TEQ/Nm³ (d.g., 11% O₂) and 1.00 is found at normal operation and with sulfur recirculation respectively (equal to a 26% reduction). A more detailed examination of the data shows that the levels of polychlorinated dibenzofurans (PCDF) were reduced with about 50% while the polychlorinated dibenzo-p-dioxin (PCDD) levels were more or less unchanged. This finding is most likely explained by the importance of the reaction rate of the de novo synthesis for the formation of PCDFs whereas the PCDDs have been shown to be rather unaffected by changes in chlorine and sulfur ratios (Aurell, 2008; Aurell et al., 2009a,b).

The mean value decreased from 1.84 to 1.57 ng I-TEQ/g in the ashes when recirculation of sulfur was employed. Polychlorinated benzenes (PCBz) were also measured in the flue gas. The mean total concentration of tri to hexachlorinated benzenes decreased

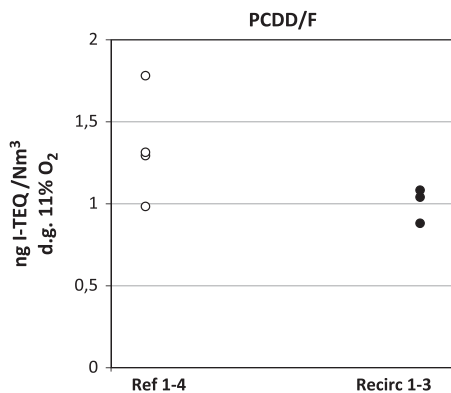


Fig. 9. Measured I-TEQ levels in the four flue gas samples taken at normal conditions (Ref) and in the three samples taken at sulfur recirculation (Recirc). Each circle represents one flue gas sample. The levels are expressed at ng I-TEQ/Nm³ d.g. @ 11%O₂.

from 2.9 μg/Nm³ (d.g., 11% O₂) (mean value of three samples) to 1.6 μg/Nm³ (d.g., 11% O₂) (mean value of two samples).

3.5. Corrosion

3.5.1. Corrosion rate

Fig. 10 shows mean values of material loss measurements on 16Mo3, Sanicro 28 and Inconel 625 samples exposed in the reference case and with sulfur recirculation at 450 °C and 525 °C (material temperatures) for 1000 h. On all materials and temperatures, a decrease in material loss was detected when sulfur recirculation was activated. At 450 °C, the greatest effect of sulfur recirculation on corrosion rate was exhibited by the low-alloyed steel 16Mo3, the decrease in corrosion rate being about 60%. The material loss for the two high-alloyed steels is significantly lower compared with 16Mo3, regardless of exposure conditions. It should be noted that the material losses are generally low at 450 °C and the measured values of the high-alloyed steels is just above the measurement uncertainty.

At 525 °C, a more drastic decrease in material loss is seen for all three steels with sulfur recirculation. The greatest effect is seen on the high-alloyed steels, where a reduction of 87% and 80% is measured for Sanicro 28 and Inconel 625 correspondingly compared with reference samples.

3.5.2. Metallographic cross sections investigated by SEM

3.5.2.1. 16Mo3. at 450 °C material temperature. The left image in Fig. 11 shows a metallographic cross section of a 16Mo3 sample exposed 1000 h at 450 °C (material temperature) in the reference case. The cross section can be divided into three parts, namely (from bottom to top) steel, corrosion product layer and deposit. Since the image is taken with a BSE detector, the contrast of the

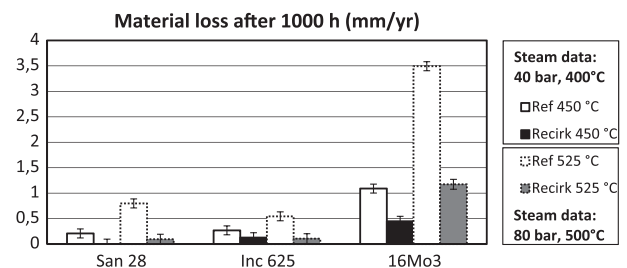


Fig. 10. Mean values of 8 material loss measurements per sample ring. The measurement uncertainty is 0.02 μm/h and is represented by the error bars. The white bars represent the reference exposure at 450 °C and 525 °C, respectively. The black and the dark gray bars represent the sulfur recirculation exposures at 450 °C and 525 °C.

image results from different elements. Heavy elements in the image are bright and lighter elements are dark. Black areas are pores and cracks filled with epoxy (consisting mostly of carbon). Beneath the deposit layer the corrosion product layer is found which is about 600 μm thick and can be divided into two parts, namely an outward-growing part and an inward growing part. These parts are approximately equal in thickness and the border between these oxide layers can be seen as a faint, slightly curved line in the image. This line marks the original metal surface of the sample ring. The outward growing oxide layer has dark spots incorporated, corresponding to deposit particles encapsulated in the corrosion product layer. In the inward growing oxide layer, no encapsulated deposit particles are detected. The corrosion product layers have detached from the underlying steel ring indicating poor adherence.

The right image in Fig. 11 shows a cross section of 16Mo3 exposed 1000 h at 450 $^{\circ}\text{C}$ (material temperature) with sulfur recirculation. Similar to the reference case, the cross section can be divided into steel, corrosion product layer and deposit. Compared to the reference exposures, a significant reduction in the thickness of the corrosion layer can be noted, which in the sulfur recirculation exposure is approximately 150 μm . Moreover, the corrosion product layer formed in the sulfur recirculation exposure is much denser and adherent to the steel ring. The corrosion product layer can, similar to the reference exposure, be divided into an inward and an outward-growing part. The deposit layer on top of the corrosion product layer is relatively homogeneous in color. However, some bright areas are seen, indicating the presence of heavy elements.

The higher corrosion rate and more severe corrosion morphology of 16Mo3 in the reference exposure may be explained with the higher chlorine load compared to the sulfur recirculation exposure. Chlorine is expected to accelerate the corrosion attack by inward diffusion through the oxide grain boundaries (as Cl^-) rendering in poor scale adherence at the metal/oxide interface as well as an increased outward diffusion of Fe^{3+} (Folkesson et al., 2011; Jonsson et al., 2011).

3.5.2.2. 16Mo3 at 525 $^{\circ}\text{C}$ material temperature. The left image in Fig. 12 shows a cross section of a 16Mo3 ring exposed for 1000 h and 525 $^{\circ}\text{C}$ in the reference case. Compared to the corresponding exposure at 450 $^{\circ}\text{C}$, the corrosion attack has become even more severe. The corrosion product layer, approximately 1000–1500 μm in thickness, is loosely attached and contains numerous voids. As in the 450 $^{\circ}\text{C}$ exposure, the oxide scale can be divided into an inward growing and an outward growing part. The original steel surface is marked in the middle of the image by a faint gray line.

In similarity to the exposure at 450 $^{\circ}\text{C}$, the sulfur recirculation results in a thinner and more compact corrosion product layer (Fig. 12 right). The thickness of the corrosion product layer is reduced to about 500 μm (compared to 1500 μm in the reference case) with sulfur recirculation. The outward growing oxide is approximately 200 μm and has deposit particles encapsulated within the scale. In contrast to the dense inward growing oxide that formed on 16Mo3 in the sulfur recirculation exposure at 450 $^{\circ}\text{C}$, the inward growing oxide formed at 525 $^{\circ}\text{C}$ shows signs of a lamellar structure. This indicates that the diffusion within

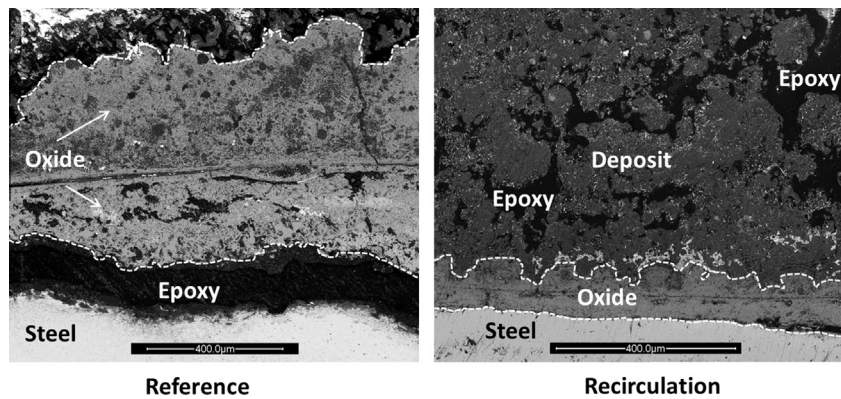


Fig. 11. SEM (BSE) images of a cross section of 16Mo3 exposed for 1000 h at 450 $^{\circ}\text{C}$ (material temperature) in the reference exposure (to the left) and in the sulfur recirculation exposure (to the right).

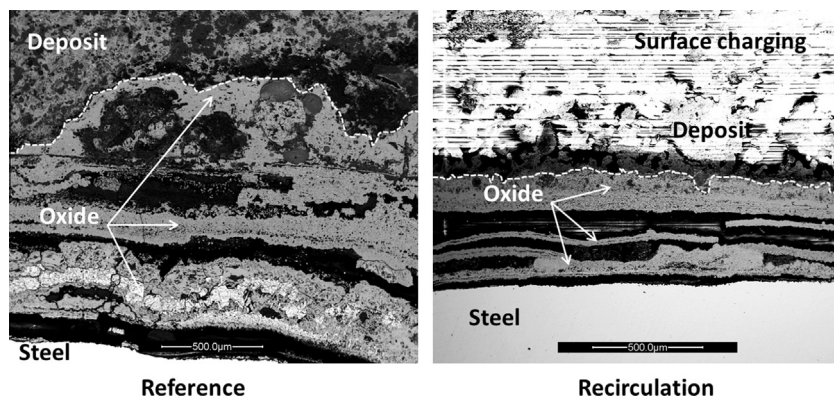


Fig. 12. SEM (BSE) images of a cross section of 16Mo3 exposed for 1000 h at 525 $^{\circ}\text{C}$ (material temperature) in the reference exposure (to the left) and in the sulfur recirculation exposure (to the right).

the oxide has been fast and large voids have formed. However, it is not clear whether this corrosion morphology arose during the exposure at high temperature or during cool down of the probe and sample preparation for SEM analysis. Hence, the large voids may have formed due to a so called pull out effect during sample preparation for SEM analysis. The bright area at the top of the image is caused by the charging of the surface during SEM analysis.

3.5.2.3. Sanicro 28 at 450 °C material temperature. The left image in Fig. 13 shows a cross section of Sanicro 28 exposed for 1000 h at 450 °C (material temperature) in the reference case. Compared to the corresponding exposure of the low alloyed 16Mo3, the corrosion attack on Sanicro 28 is not equally severe. The corrosion product layer formed is approximately 70 µm thick (compared to 600 µm in the case of 16Mo3) and a faint, somewhat undulating, line is seen in the middle of the oxide scale, indicating the presence of the former sample surface. The oxide scale is rather homogenous and well adherent to the steel. The deposit layer on top of the corrosion product layer is not entirely homogeneous and some dark areas can be seen. These areas are pores and even after 1000 h of exposure the deposit layer is not completely sealed.

The image to the right in Fig. 13 shows a cross section of a Sanicro 28 sample exposed 1000 h at 450 °C (material temperature) with sulfur recirculation. In this exposure, Sanicro 28 is able to withstand the corrosive environment during the 1000 h and the thin oxide formed is protective and well adherent. The deposit layer formed on top of the oxide is, compared to the corresponding deposit formed in the reference exposure, relatively homogenous

but not equally dense. Some dark areas (epoxy) can be seen as well as some, almost, white areas (in the upper left corner). The white areas indicate the presence of heavy metals.

The deposit layer formed on Sanicro 28 in the sulfur recirculation exposure is dominated by sulfate containing compounds and thus, the protective oxide initially formed remains intact. In the reference exposure, the deposit contains higher amounts of alkali chlorides and the protective oxide is depleted in chromium by the formation of alkali chromates and thereby its protective properties. This also opens up for further corrosion attack by chlorine. The mitigating effect of sulfating alkali chlorides and alkali carbonates into corresponding alkali sulfates on corrosion has been shown in the laboratory (Pettersson et al., 2011).

3.5.2.4. Sanicro 28 at 525 °C material temperature. The left image in Fig. 14 shows a cross section of Sanicro 28 exposed for 1000 h at 525 °C in the reference case. The increase in material temperature from 450 °C to 525 °C results in a corrosion product growth of Sanicro 28. At 525 °C, the corrosion attack ranges from 150 to 400 µm, compared to roughly 70 µm thickness of the corrosion product layer in the corresponding exposure at 450 °C. The corrosion product layer formed at 525 °C has a lamellar and porous structure and is not considered to be protective.

The right image in Fig. 14 shows a cross section of Sanicro 28 exposed for 1000 h at 525 °C with sulfur recirculation. Compared to the corresponding reference exposure, the extent of the corrosion attack is strongly decreased. The original metal surface is indicated by a faint line, running through the middle of the corrosion

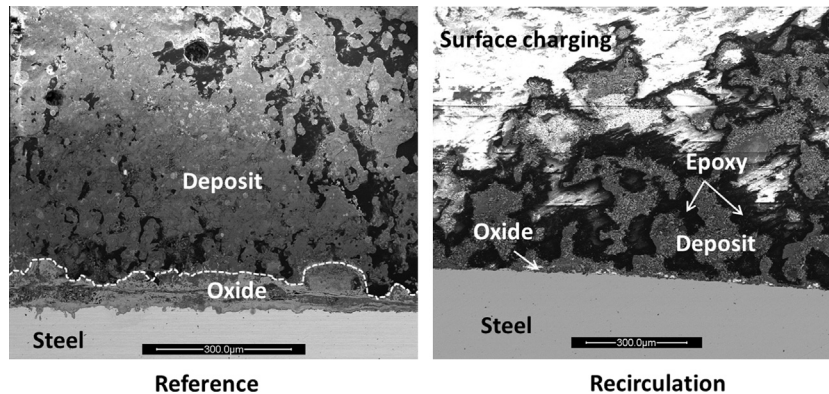


Fig. 13. SEM (BSE) images of a cross section of Sanicro 28 exposed for 1000 h at 450 °C (material temperature) in the reference exposure (to the left) and in the sulfur recirculation exposure (to the right).

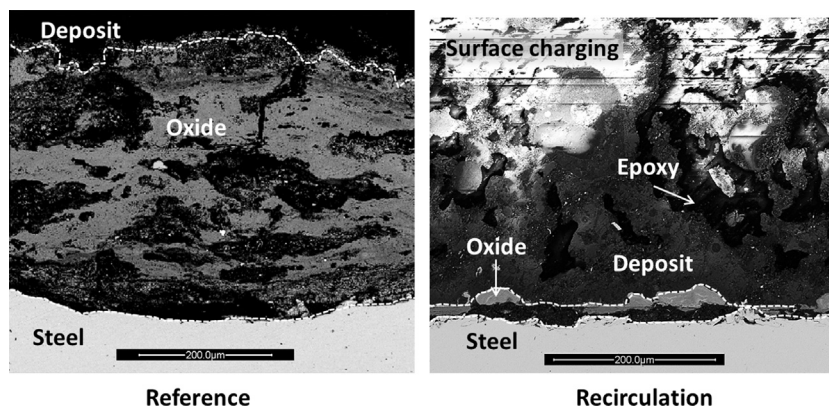


Fig. 14. SEM (BSE) images of a cross section of Sanicro 28 exposed for 1000 h at 525 °C (material temperature) in the reference exposure (to the left) and in the sulfur recirculation exposure (to the right).

product layer. The outer part of the oxide scale, *i.e.* above the faint line, is outward-growing and the oxide below is inward-growing. In some areas, a void is detected beneath the oxide scale.

3.5.2.5. Inconel 625 at 450 °C material temperature. The left image in Fig. 15 shows a cross section of Inconel 625 exposed for 1000 h at 450 °C (material temperature) in the reference case. The corrosion attack of Inconel 625 at 450 °C has not resulted in a thick continuous corrosion product layer. Instead, only localized areas with thicker corrosion products were detected. Above the corrosion front, a 400 µm thick inner deposit layer can be seen. This deposit layer contains some voids but is overall rather dense. Above this layer a somewhat brighter deposit layer is seen. This layer contains few voids and is, according to the morphology and the BSE contrast, fairly homogenous in composition. Due to the higher chromium content in the oxide on Inconel 625 compared to Sanicro 28, the nickel base material, Inconel 625, is able to withstand the corrosive environment in the reference exposure at 450 °C slightly better.

The right image in Fig. 15 shows a cross section of Inconel 625 exposed for 1000 h at 450 °C (material temperature) with sulfur recirculation. In similarity to the Sanicro 28 sample, the corrosion rate of Inconel 625 is low. In fact, Inconel 625 does not show any signs of accelerated corrosion attack during 1000 h exposure at 450 °C when sulfur recirculation is active. The evenness of the steel ring surface indicates that the oxide formed is protective and less than a couple of microns thick. In contrast to the reference case no areas with local corrosion attack are detected. The deposit

formed on the sample ring in the sulfur recirculation case is fairly porous.

3.5.2.6. Inconel 625 at 525 °C material temperature. The left image in Fig. 16 shows a cross section of Inconel 625 exposed for 1000 h at 525 °C in the reference case. The image reveals a rather thick corrosion product layer, roughly 450 µm in thickness. This layer contains large voids and has a lamellar structure. Dark and bright areas are distinguished, indicating that the corrosion layer is heterogeneous in its structure. Above the corrosion product layer a mixed oxide/deposit layer is seen, about 100–400 µm in thickness is detected. The incorporation of deposit particles in the oxide matrix suggests that this layer is outward growing, and thus, the oxide scale beneath is inward growing. Even though Inconel 625 forms rather pure Cr₂O₃, the increase in temperature from 450 °C to 525 °C in this corrosive environment with abundance of alkali chlorides lead to a failure of the protective oxide.

The right image in Fig. 16 shows the cross section of Inconel 625 exposed for 1000 h at 525 °C with sulfur recirculation. The deposit layer is apparently porous and composed of small incoherent particles. The conductivity of the deposit is poor and thus, charge effects can be detected in the microscope. Beneath the deposit layer, no corrosion product layer could be seen (at the current magnification). The increase of material temperature, from 450 to 525 °C, was apparently not enough to accelerate the corrosion attack. Inconel 625 is expected to be protected by a thin and chromium-rich oxide in the sulfur recirculation exposures at 450 °C and 525 °C.

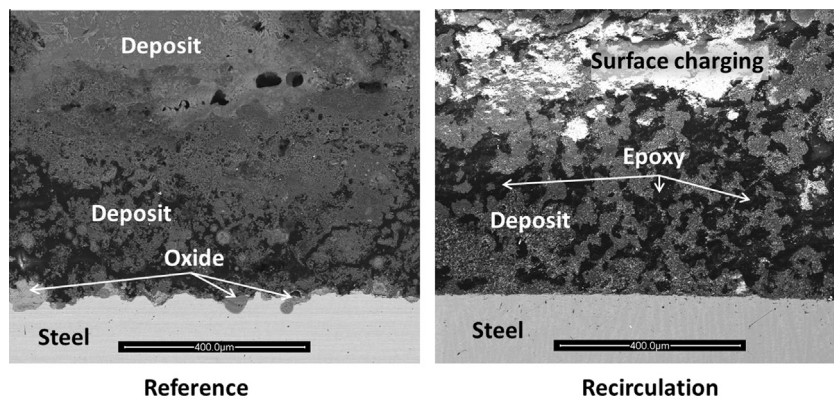


Fig. 15. SEM (BSE) images of a cross section of Inconel 625 exposed for 1000 h at 450 °C (material temperature) in the reference exposure (to the left) and in the sulfur recirculation exposure (to the right).

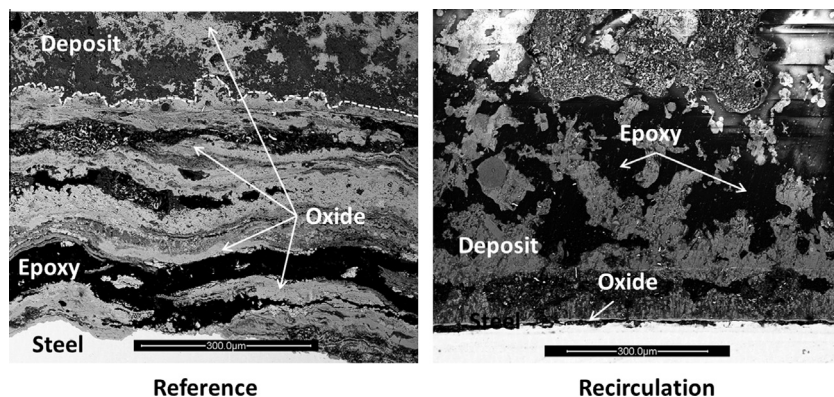


Fig. 16. SEM (BSE) images of a cross section of Inconel 625 exposed for 1000 h at 525 °C (material temperature) in the reference exposure (to the left) and in the sulfur recirculation exposure (to the right).

4. Conclusions

The general conclusion of this work is that the sulfur recirculation process can be installed in existing and new Waste-to-Energy plants and biomass fired boilers with wet flue gas cleaning. Sulfur recirculation has the potential to increase steam data and electricity production from MSWI (Municipal Solid Waste Incineration) without increasing the corrosion rate of the superheaters. As an alternative, the corrosion rate can be significantly reduced if the superheaters are operated at the same temperature. More specific conclusions to be drawn from the full-scale demonstration of sulfur recirculation are:

4.1. Sulfur recirculation

A high, relatively constant SO₂ concentration could be maintained by sulfur recirculation, in contrast to normal operation which was characterized by strong fluctuation and periods of very low SO₂ concentrations. The high SO₂ concentration was achieved by a control loop, where the sulfuric acid dosage to the boiler was controlled by the SO₂ gas concentration downstream of the boiler. Acid dew point measurements showed no increased risk for low temperature corrosion.

No negative impact on the emissions was measured during sulfur recirculation. The emissions of SO₂, HCl, NO_x and TOC were not changed significantly while NH₃ and CO emissions decreased.

4.2. The influence of sulfur on ashes and deposits

Due to the higher sulfation rates at increased SO₂ concentrations, sulfur recirculation increased the sulfur concentration in the fly ash and boiler ash, which acted as a sulfur sink. There is a potential for sulfate waste water free operation, thus eliminating the need for gypsum precipitation process in some plants. More chlorides are discharged with the effluent water to the recipient (normally the sea) and less chlorides are landfilled due to the sulfation of the alkali chlorides. The costs for boiler cleaning has a potential to decrease since the deposit growth decreased by one third.

4.3. The influence of sulfur on dioxins

The sulfation of the ashes and deposits during sulfur recirculation lead to a decrease in dioxin formation. The dioxin concentration (I-TEQ) of the flue gas was reduced by approximately 25% and Polychlorinated benzenes (PCBz) in the flue gas decreased by approximately 50%. A slight decrease in dioxin concentration (I-TEQ) was also found in the fly ash.

4.4. The influence of sulfur on corrosion

The corrosion rate decreased significantly for all investigated materials (16Mo3, Sanicro 28 and Inconel 625) compared to the reference exposures. The cost for replacing superheaters is therefore reduced. With sulfur recirculation, the material temperature could be raised 75 °C at similar or even lower corrosion rates, which allows for higher steam parameters and electrical efficiency.

The corrosion morphology of the samples in the sulfur recirculation exposure was different compared to the samples exposed in the reference case. Sulfur recirculation prevented the formation of transition metal chlorides at the metal/oxide interface, formation of chromate and reduced the presence of zinc in the corrosion products.

Acknowledgements

The helpful staff at Renova and the financial support from WasteRefinery and ProEnviro are gratefully acknowledged.

References

- Asteman, H., Svensson, J.E., Johansson, L.G., Norell, M., 1999. Indication of chromium oxide hydroxide evaporation during oxidation of 304L at 873 K in the presence of 10% water vapor. *Oxid. Met.* 52 (1–2), 95–111.
- Aurell, J., 2008. Effects of Varying Combustion Conditions on PCDD/F formation. Doctoral Thesis, Department of Chemistry, Umeå University, Sweden.
- Aurell, J., Fick, J., Haglund, P., Marklund, S., 2009a. Effects of varying combustion conditions on PCDD/F emissions and formation during MSW incineration. *Chemosphere* 75, 667–673.
- Aurell, J., Fick, J., Haglund, P., Marklund, S., 2009b. Effects of sulfur on PCDD/F and PCDT formation under stable and transient combustion conditions during MSW incineration. *Chemosphere* 76, 767–773.
- Becker, E., Reinmann, J., Rentschler, W., Mayer, J., 2000. Continuous monitoring of the dioxin/furan emission of all waste incinerators in Belgium. *Organohalogen Comp.* 49S, 21–23.
- Bøjer, M., Arendt Jensen, P., Frandsen, F., Dam-Johansen, K., Hedegaard-Madsen, O., Lundtorp, K., 2008. Alkali/chloride release during refuse incineration on a grate: full-scale experimental findings. *Fuel Process. Technol.* 89, 528–539.
- Brostrom, M., Kassman, H., Helgesson, A., Berg, M., Andersson, C., Backman, R., Nordin, A., 2007. Sulfation of corrosive alkali chlorides by ammonium sulfate in a biomass fired CFB boiler. *Fuel Process. Technol.* 88 (11–12), 1171–1177.
- Chang, M.B., Cheng, Y.C., Chi, K.H., 2006. Reducing PCDD/F formation by adding sulfur as inhibitor in waste incineration process. *Sci. Total Environ.* 366, 456–465.
- Davidsson, K., Amand, L.E., Steenari, B.M., Elled, A.-L., Eskilsson, D., Leckner, B., 2008. Countermeasures against alkali-related problems during combustion of biomass in a circulating fluidized bed boiler. *Chem. Eng. Sci.* 63, 5314–5329.
- Folkesson, N., Pettersson, J., Pettersson, C., Johansson, L.-G., Skog, E., Svensson, J.-E., 2008. Fireside corrosion of stainless and low alloyed steels in a waste-fired CFB boiler, the effect of adding sulphur to the fuel. *Mater. Sci. Forum* 595–598, 289–297.
- Folkesson, N., Jonsson, T., Halvarsson, M., Johansson, L.-G., Svensson, J.-E., 2011. The influence of small amounts of KCl(s) on the high temperature corrosion of a Fe-2.25Cr-1Mo steel at 400 and 500 °C. *Mater. Corros.* 62 (7), 606–615.
- Froitzheim, J., Ravash, H., Larsson, E., Johansson, L.G., Svensson, J.E., 2010. Investigation of chromium volatilization from FeCr interconnects by a Denuder technique. *J. Electrochem. Soc.* 157 (9), B1295–B1300.
- Glarborg, P., Marshall, P., 2005. Mechanism and modelling of the formation of gaseous alkali sulfates. *Combust. Flame* 141, 22–39.
- Griffin, R.D., 1986. A new theory of dioxin formation in municipal solid waste combustion. *Chemosphere* 15, 1987–1999.
- Gullett, B.K., Bruce, K.R., Beach, L.O., 1992. Effect of sulfur dioxide on the formation mechanism of polychlorinated dibenzodioxin and dibenzofuran in municipal waste combustion. *Environ. Sci. Technol.* 26, 1943–1983.
- Gullett, B.K., Dunn, J.E., Raghunathan, K., 2000. Effect of cofiring coal on the formation of polychlorinated dibenzo-p-dioxin and polychlorinated dibenzofurans during waste combustion. *Environ. Sci. Technol.* 34, 282–290.
- Halvarsson, M., Tang, J.E., Asteman, H., Svensson, J.-E., Johansson, L.-G., 2006. Microstructural investigation of the breakdown of the protective oxide scale on a 304 steel in the presence of oxygen and water vapour at 600 °C. *Corros. Sci.* 48 (8), 2014–2035.
- Hindiyarti, L., Frandsen, F., Livbjerg, H., Glarborg, P., Marshall, P., 2008. An exploratory study of alkali sulfate aerosol formation during biomass combustion. *Fuel* 87, 1591–1600.
- Hunsinger, H., Seifert, H., Jay, K., 2003. Formation of PCDD/F during start-up of MSWI. *Organohalogen Comp.* 63, 37–40.
- Hunsinger, H., Seifert, H., Jay, K., 2006. An economic process to inhibit PCDD/F formation in MSWI by SO₂. *Organohalogen Comp.* 68, 151–156.
- Hunsinger, H., Seifert, H., Jay, K., 2007. Reduction of PCDD/F formation in MSWI by a process-integrated SO₂ cycle. *Environ. Eng. Sci.* 24, 1145–1159.
- Li, K., Lu, Y., Salmenoja, K., 1999. Sulfation of potassium chloride at combustion conditions. *Energy Fuels* 13, 1184–1190.
- Jardnas, A., Svensson, J.-E., Johansson, L.-G., 2001. Evidence for suppression of the oxidation of a Fe 2.25Cr 1 Mo steel by traces of SO₂. *Mater. Sci. Forum* 369–3, 173–180.
- Jardnas, A., Svensson, J.-E., Johansson, L.-G., 2008. Influence of SO₂ on the oxidation of 304L steel in O₂ + 40% H₂O at 600 °C. *Oxid. Met.* 69 (3–4), 249–263.
- Johansson, L., Leckner, B., Tullin, C., Amand, L.E., Davidsson, K., 2008. Properties of particles in the fly ash of a biofuel-fired circulating fluidized bed (CFB) boiler. *Energy Fuels* 22, 3005–3015.
- Jonsson, T., Froitzheim, J., Pettersson, J., Svensson, J.E., Johansson, L.G., Halvarsson, M., 2009. The influence of KCl on the corrosion of an austenitic stainless steel (304L) in oxidizing humid conditions at 600 °C: a microstructural study. *Oxid. Met.* 72 (3–4), 213–239.
- Jonsson, T., Folkesson, T., Svensson, J.E., Johansson, L.G., 2011. An ESEM in-situ investigation of initial stages of the KCl induced high temperature corrosion of a Fe-2.25Cr-1Mo steel at 400 °C. *Corros. Sci.* 53 (6), 2233–2246.

- Kassman, H., Pettersson, J., Steenari, B.M., Amand, L.E., 2013. Two strategies to reduce gaseous KCl and chlorine in deposits during biomass combustion— injection of ammonium sulphate and co-combustion with peat. *Fuel Process. Technol.* 105, 170–180.
- Lang, T., Arendt Jensen, P., Nygaard Knudsen, J., 2006. The effects of Ca-based sorbents on sulfur retention in bottom ash from grate-fired annual biomass. *Energy Fuels* 20, 796–806.
- Lindbauer, R.L., Wurst, F., 1992. Combustion dioxin suppression in municipal solid waste incineration with sulphur additives. *Chemosphere* 25, 1409–1414.
- Miles, T.R., Baxter, L.L., Bryers, R.W., Jenkins, B.M., Oden, L.L., 1996. Boiler deposits from firing biomass fuels. *Biomass Bioenergy* 10, 125–138.
- Ogawa, H., Orita, N., Horaguchi, M., Suzuki, T., Okada, M., Yasuda, S., 1996. Dioxin reduction by sulfur component addition. *Chemosphere* 32, 151–157.
- Olsson, J., Jaglid, U., Pettersson, J.B.C., Hald, P., 1997. Alkali metal emission during pyrolysis of biomass. *Energy Fuels* 11, 779–784.
- Pettersson, J., Asteman, H., Svensson, J.-E., Johansson, L.-G., 2005. KCl induced corrosion of a 304-type austenitic stainless steel at 600 °C. *Role Potass. Oxid. Met.* 64 (1–2), 23–41.
- Pettersson, C., Pettersson, J., Asteman, H., Svensson, J.-E., Johansson, L.-G., 2006. KCl-induced high temperature corrosion of the austenitic Fe–Cr–Ni alloys 304L and Sanicro 28 at 600 °C. *Corros. Sci.* 48 (6), 1368–1378.
- Pettersson, J., Pettersson, C., Folkeson, N., Johansson, L.-G., Skog, E., Svensson, J.E., 2006. The influence of sulphur additions on the corrosive environment in a waste-fired CFB boiler. *Mater. Sci. Forum* 522–523, 563–570.
- Pettersson, J., Folkeson, N., Johansson, L.-G., Svensson, J.-E., 2011. The effects of KCl, K₂SO₄, and K₂CO₃ on the high temperature corrosion of a 304-type austenitic stainless steel. *Oxid. Met.* 76 (1), 93–109.
- Robinson, A.L., Junker, H., Baxter, L.L., 2002. Pilot-scale investigation of the influence coal-biomass cofiring on ash deposition. *Energy Fuels* 16, 343–355.
- Ryan, P.S., Li, X.D., Gullett, B.K., Lee, C.W., Clayton, M., Touati, A., 2006. Experimental study on the effect of SO₂ on PCDD/F emissions: determination of the importance of gas-phase versus solid-phase reactions in PCDD/F formation. *Environ. Sci. Technol.* 40, 7040–7047.
- Segerdahl, K., Svensson, J.-E., Johansson, L.-G., 2002. The high temperature oxidation of 11% chromium steel: Part I – influence of pH₂O. *Mater. Corros.* 53, 247–255.
- Segerdahl, K., Pettersson, J., Svensson, J.-E., Johansson, L.-G., 2004. Is KCl(g) corrosive at temperatures above its dew point? – influence of KCl(g) on initial stages of the high temperature corrosion of 11% Cr steel at 600 °C. *Mater. Sci. Forum* 461–464, 109–116.
- Theis, M., Skrifvars, B.J., Zevenhoven, M., Hupa, M., Tran, H.H., 2006. Fouling tendency of ash resulting from burning mixtures of biofuels. Part 2: deposit chemistry. *Fuel* 85, 1992–2001.
- Viklund, P., Pettersson, R., Hjörnhede, A., Henderson, P., Sjövall, P., 2009. Effect of sulphur containing additive on initial corrosion of superheater tubes in waste fired boiler. *Corros. Eng. Sci. Technol.* 44 (3), 234–240.
- Wikström, E., Ryan, S., Touati, A., Telfer, M., Tabor, D., Gullett, B., 2003. Importance of chlorine speciation on de novo formation of polychlorinated dibenzo-p-dioxins and dibenzofurans. *Environ. Sci. Technol.* 37, 1108–1113.